Supplement of Hydrol. Earth Syst. Sci., 30, 1849–1864, 2026
https://doi.org/10.5194/hess-30-1849-2026-supplement

Hydrology and Earth System Sciences
Open Access
EGU

Supplement of

Increasing glacier runoff in northwestern Greenland simulated from 1950 to 2023

Ken Kondo and Koji Fujita

Correspondence to: Ken Kondo (kenkondo0410@gmail.com)

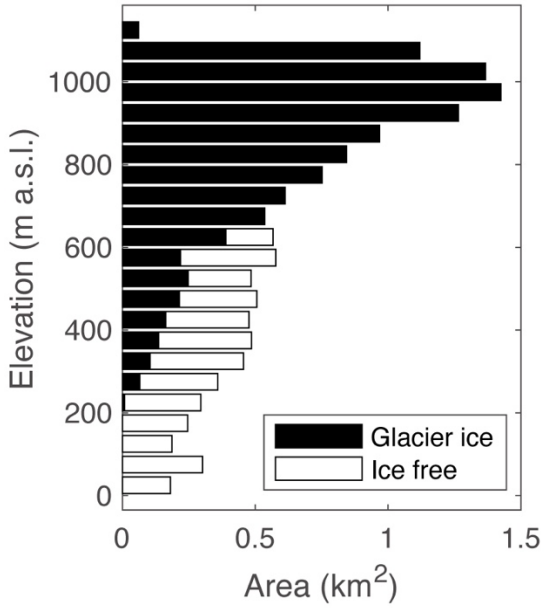

Figure S1: Hypsometry of the catchment area of the outlet stream from Qaanaaq Glacier partitioned into glacier-covered (black) and ice-free (white) areas.

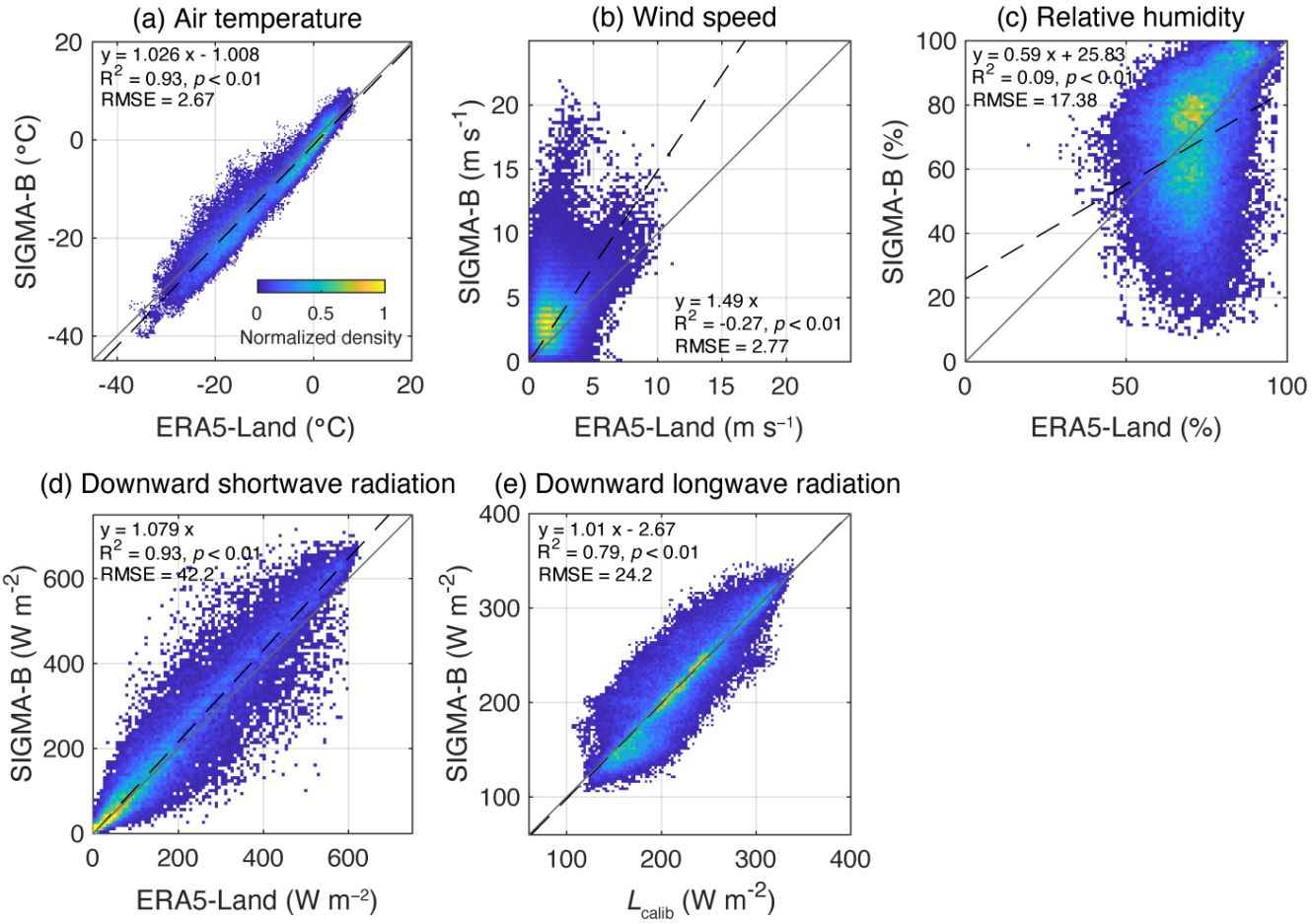

Figure S2: Comparisons of the ERA5-Land data (horizontal axes) and observations at SIGMA-B (vertical axes) with density plots for (a) air temperature, (b) wind speed, (c) relative humidity, (d) downward shortwave radiation, and (c) downward longwave radiation (L_{calib}). The dashed line indicates a linear regression through the data. The linear regression equation is shown along with the coefficient of determination (R^2) and RMSE.

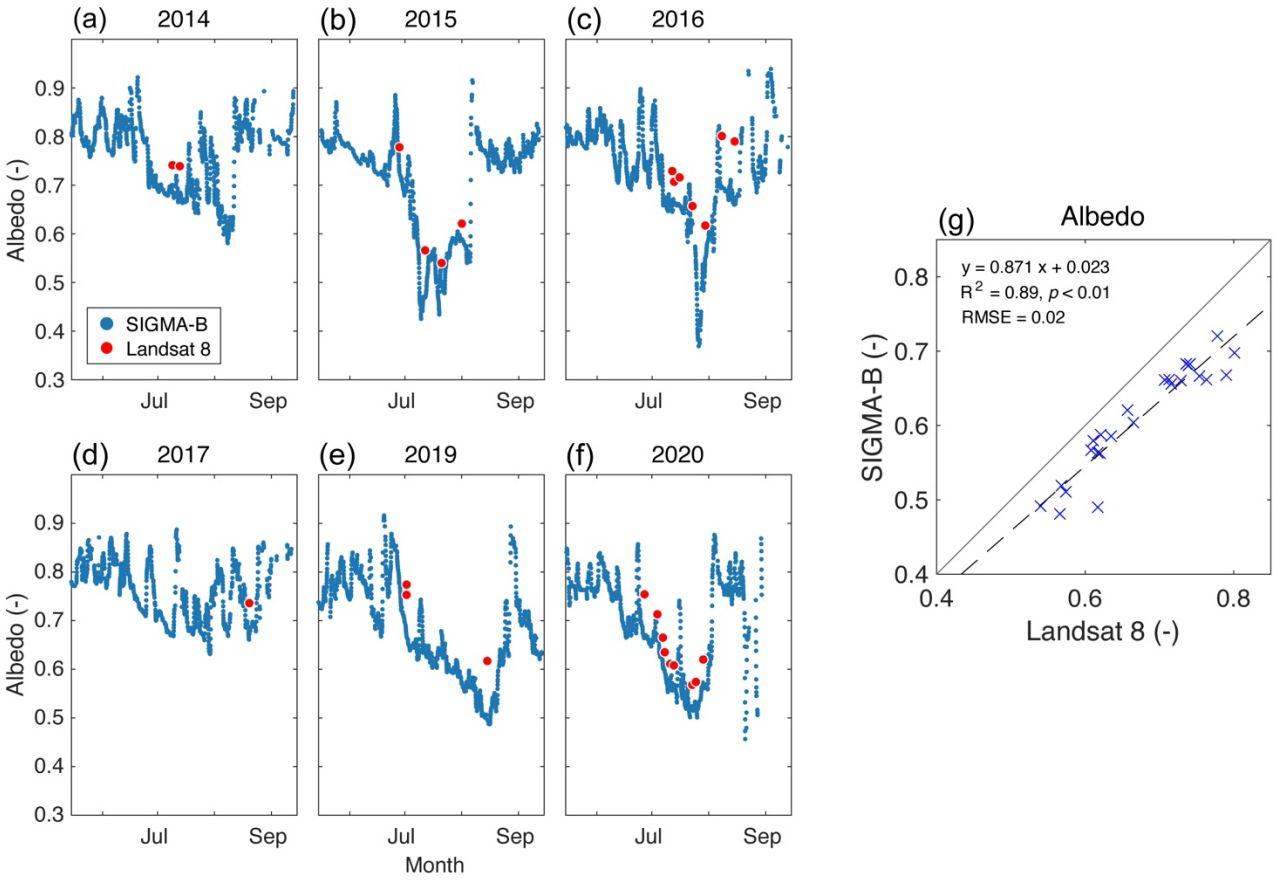

Figure S3: (a–f) Surface albedo observed at the SIGMA-B site by AWS (blue) and Landsat 8 (red) in 2014–2020. (g) Plot of the surface albedo observed by SIGMA-B AWS and Landsat 8. The linear regression equation is shown along with the coefficient of determination (R^2) and RMSE.

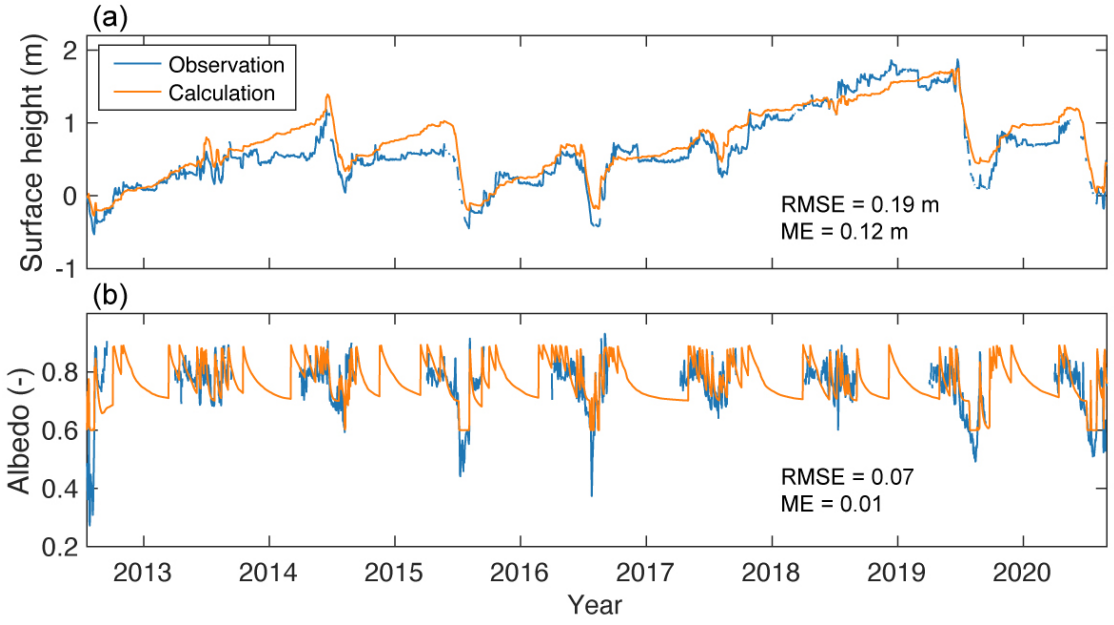

Figure S4: (a) Observed (blue) and calculated (orange) surface height changes and (b) albedo at the SIGMA-B site. The RMSE and ME are also shown.

20

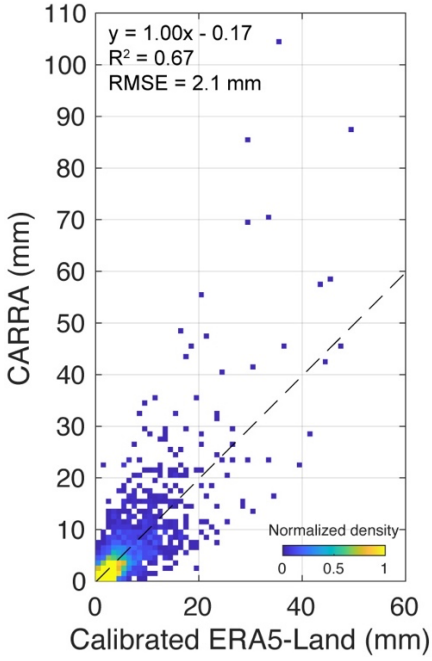

Figure S5: Daily precipitation in 1991–2023 from calibrated ERA5-Land versus CARRA reanalysis data with a density plot. The dashed line indicates a linear regression through the data. The linear regression equation is shown along with the coefficient of determination (R^2) and RMSE.

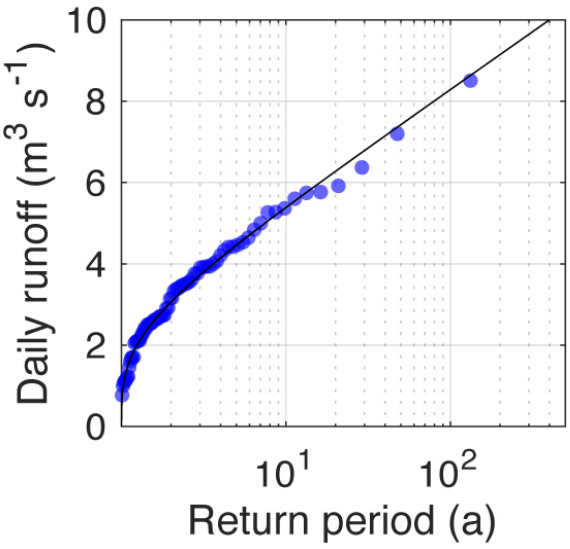

Figure S6: Return periods for the calculated daily runoff (circles) and cumulative distribution function of the fitted Gumbel distribution (black line).

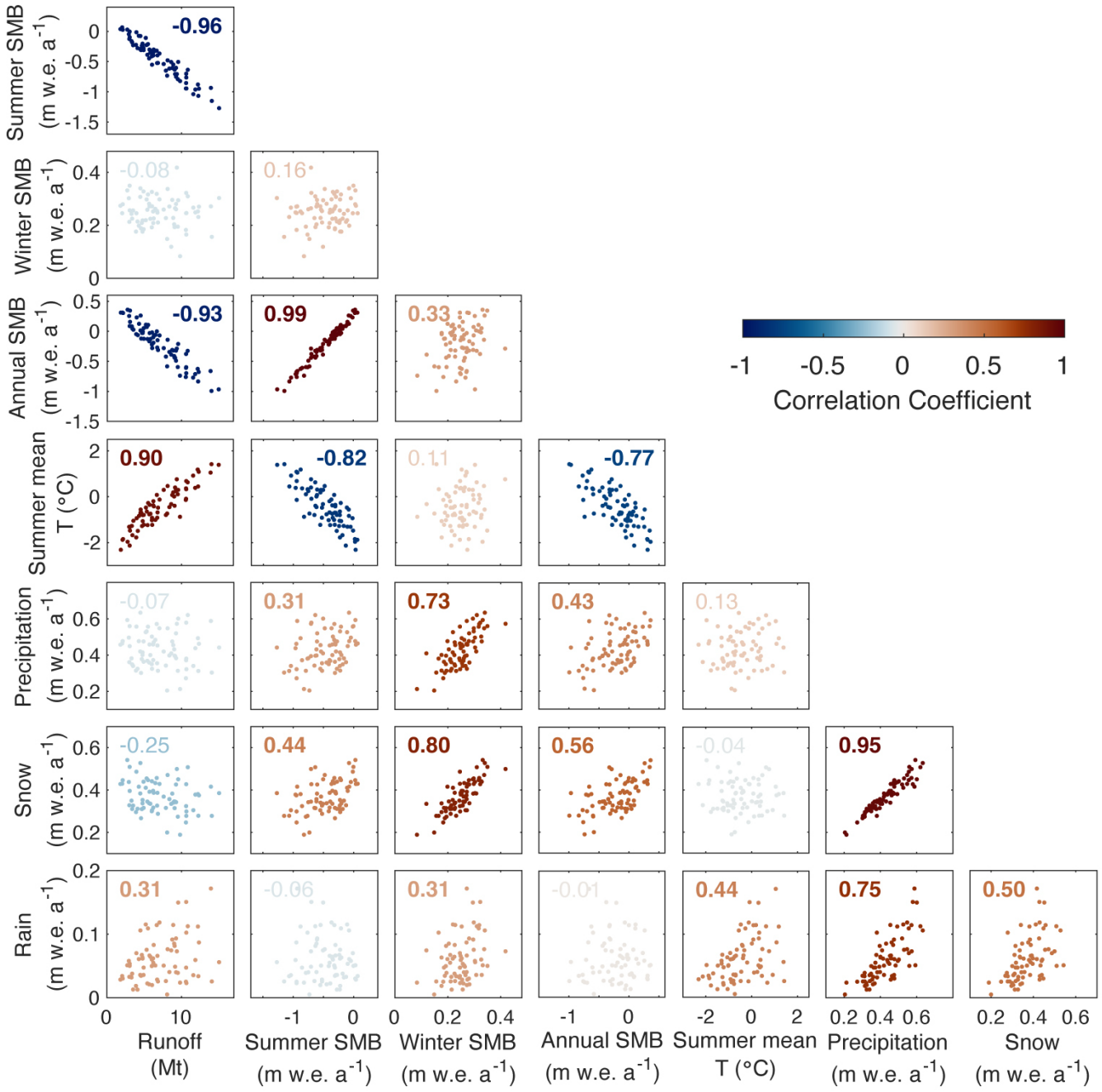

Figure S7: Scatter plots and correlation coefficients for the model results and meteorological conditions shown in Fig. 6. The text and colors show the correlation coefficients. Bold text indicates correlations with $p < 0.01$.

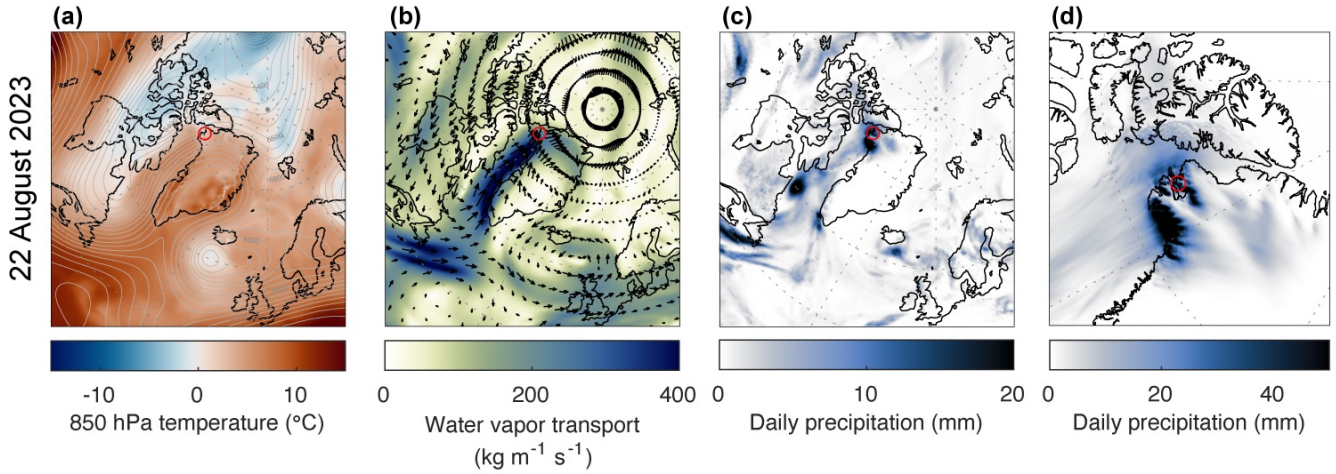

Figure S8: ERA5 (a–c) and CARRA (d) reanalysis data for 22 August 2023. (a) Air temperature at 850 hPa geopotential (color) and height at 500 hPa geopotential (gray contours). (b) Vertically integrated water vapor transport (color) and wind vectors at 850 hPa geopotential (arrows). (c) Daily precipitation from ERA5. (d) Daily precipitation from CARRA. The red circles indicate the location of Qaanaaq.

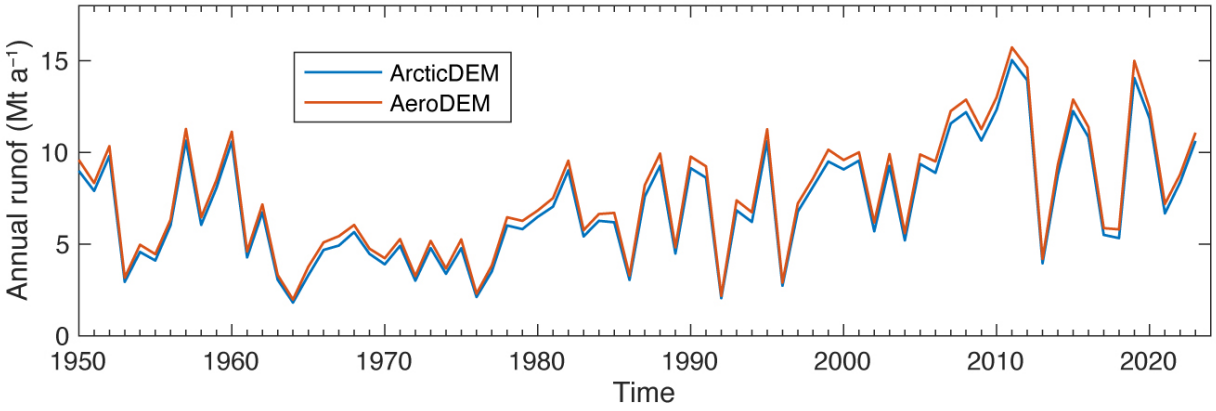

Figure S9: Annual runoff calculated using the area–altitude distribution derived from ArcticDEM Mosaic (blue) and AeroDEM (orange), based on data acquired in 2007–2022 and 1985, respectively.

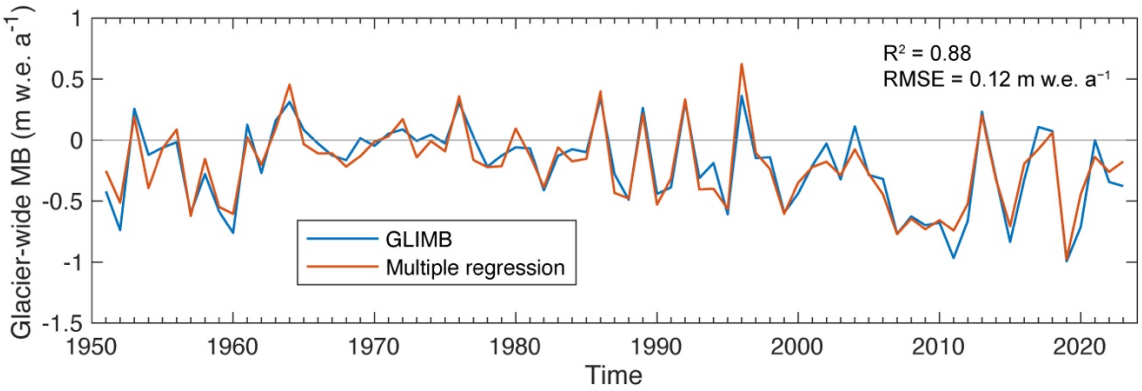

Figure S10: Glacier-wide mass balance from GLIMB (blue) and multiple regression analysis using the air temperature and snowfall (orange). The coefficient of determination (R^2) and RMSE of the regression are given.

50

Table S1: Results of multiple regression analysis for estimating the annual glacier mass balance (m w.e. a^{-1}) using summer mean air temperature and snowfall.

	Estimate	Standard error	t-Stat	$p <$
Intercept	−1.21	0.07	−17.9	0.001
Summer mean air temperature (°C)	−0.29	0.02	−18.2	0.001
Snowfall (m w.e. a^{-1})	2.20	0.17	13.1	0.001

55

Table S2: Five years with the highest and lowest summer GBI and their values used for the atmospheric composite analysis shown in Fig. 9.

	Year	Summer GBI (m)
High-GBI period	2019	5567
	2012	5564
	2016	5547
	2011	5545
	2007	5543
Low-GBI period	1972	5448
	1994	5449
	1983	5451
	1976	5457
	1992	5483